ANALYSIS OF FLOW THROUGH A DOUBLE-ACTING IMPELLER WITH A STRAIGHT RADIAL BLADES USING CFD

SUTHEP KAEWNAI

Department of Mechanical Engineering, Faculty of Engineering, King Mongkut's University of Technology Thonburi, Bangmod, Bangkok 10140, Thailand, suthep.kae@kmutt.ac.th

Somchai Wongwises
King Mongkut's University of Technology Thonburi, somchai.won@kmutt.ac.th

ANALYSIS OF FLOW THROUGH A DOUBLE-ACTING IMPELLER WITH A STRAIGHT RADIAL BLADES USING CFD

SUTHEP. KAEWNAI[1], SOMCHAI WONGWISES[2]

[1,2]Fluid Mechanics, Thermal Engineering and Multiphase Flow Research Lab. (FUTURE), Department of Mechanical Engineering, Faculty of Engineering, King Mongkut's University of Technology Thonburi, Bangmod, Bangkok 10140, Thailand
Corresponding author: E-mail: Suthep.kae@kmutt.ac.th[1], somchai.won@kmutt.ac.th[2]

Abstract- This study aims to analyze water flow through a centrifugal pump with straight radial blades double-acting impeller using computational fluid dynamics (CFD). The impeller analyzed was designed with the following conditions: a volume flow rate of 33.5 m^3/h, head of 100 m, rotational speed of 2,950 rpm, and specific speed of 9. The first stage began with calculations for various dimensions of double-acting isolated impeller and impeller-collector assembly, followed by three-dimensional drawing and domain specification. In the second stage, grids for the isolated impeller and impeller-collector assembly were generated. In the third stage, the initial conditions and boundary conditions were specified. Finally, the water flow through the isolated impeller and impeller-collector assembly was analyzed using the CFX 13 code to predict the water flow state. A fluid dynamic analysis of the isolated impeller and impeller-collector assembly reveals that the Q-H curve rises continuously toward shutoff as the flow rate is reduced. The results indicate that the total head rise of the isolated impeller is approximately 98.8 m for a 65 mm impeller inlet width and 99.89 m for a 70 mm impeller inlet width. This may be due to reduced circulation between blade passages of impeller. Similar to the isolated impeller, the Q-H curve of the impeller-collector assembly also rises continuously toward shutoff as the flow rate is reduced. The total head rise is reduced to approximately 98 m because of losses in the collector. Concerning the flow in the impeller-collector assembly when Q/Q_{design} is or less than 1.0, the pressure distribution is high at the tongue of collector. Concerning the velocity distribution when Q/Q_{design} is more or less than 1.0, there is circulation or a vortex at the top of the collector.

Keyword- *Double acting, blade, impeller, specific speed*

I. INTRODUCTION

The potential of computational fluid dynamics (CFD) for the design of centrifugal pumps has not been extensively exploited in the pump industry. Many types of pumps continue to be designed using empirical principles and techniques by means of one-dimensional flow analysis or simple tests. These have a limitation in accurate performance prediction and cannot contribute to improvement by considering three-dimensional flow. The key advantage of CFD analysis is that it can be used as a numerical test bed that can minimize the required testing and costs for the development of new products and also offers the support for the design optimization of existing configurations. The applications of CFD in pumps have been studied by a number of researchers [1],[2], [5-8]. M. Asujie et al. [1] performed a 3D-CFD simulation of the impeller and volute of a centrifugal pump with a specific speed of 32 (metric units) using CFX code. A 3D flow simulation for an impeller with structured grids was presented. Muggli et al. [2] showed good agreement between simulation and experimental results.

Although some information is currently available on applying CFD for the prediction of radial flow type impellers, but no researchers have applied it in predicting stability and other features in double-acting impeller with straight radial blades for a centrifugal pump.

A. Overview of double-acting impeller with straight radial blades

According to Croper et al. [3], many processes in the hydrocarbon processing industry require pumps that deliver high heads at low flows. To reach high heads, either the pump has to operate above synchronous speed or the impellers need to have large diameters and very small flow passages. The former solution usually requires gear-driven pumps with inducer-type hydraulics to manage the suction requirements. The latter solution leads to large impellers with narrow passages, which require special casting techniques to reliably reach performance goals. A centrifugal pump with double-acting impeller geometry can avoid these disadvantages.

A double-acting impeller with straight radial blades is shown in Fig. 1. The impeller is used in a single-stage, single-entry centrifugal pump. The head achieved is above 300 m [3], [4]. Nearly identical blades are arranged on both sides of the center rib. The large opening in the center rib near the hub allows half of the fluid to flow to the blades in the rear. The impeller is used for pumps in the range of about $1 < n_q < 10$. The shape of the head capacity, or the Q-H curve, of a centrifugal pump has a major

impact on reliable operation of the pump. A Q-H curve rising continuously toward shutoff as the flow rate is reduced is considered stable. An unstable Q-H curve can be drooping toward shutoff or have a saddle. In a double-acting impeller with straight blades for centrifugal pumps, Q-H curves are stable because of the high head coefficient. Due to the low blade loading, vibrations are very low.
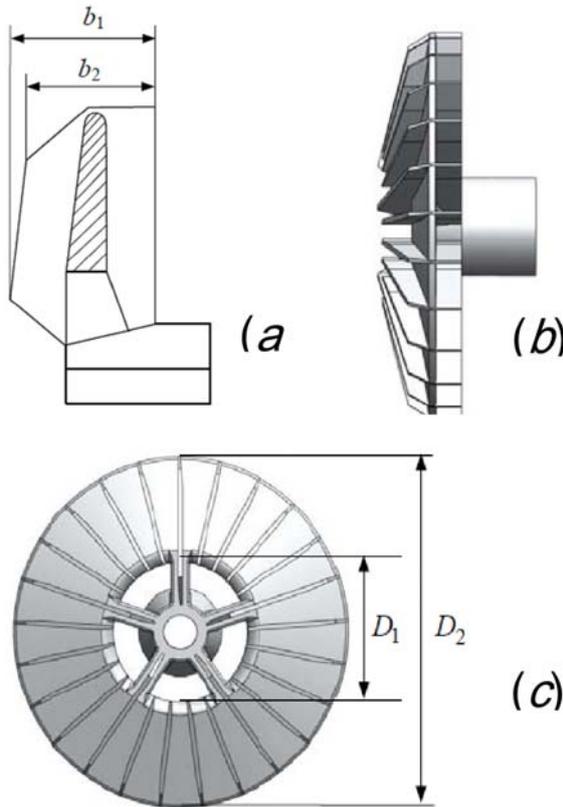

Fig.1. Double-acting impeller with straight radial blades

II. ONE-DIMENSIONAL DESIGN OF THE IMPELLER

Initially, the specifications of the impeller were established. The volume flow rate (Q), total head (H), and rotational speed (n) were defined. The one-dimensional preliminary was focused on the BEP (best efficiency point).

A. Basic equation for impeller design and performance

Specific speed: $n_q = \dfrac{n\sqrt{Q}}{H^{3/4}}$ (1)

Head coefficient: $\psi = \dfrac{2gH}{u_2^2}$ (2)

Flow coefficient : $\phi = \dfrac{C_{2m}}{u_2}$ (3)

Circumferential impeller velocity: $u = \dfrac{\pi n D}{60}$ (4)

Impeller width: $b = \dfrac{Q}{\pi D C_m}$ (5)

Circumferential component of absolute velocity:

$C_u = u - \dfrac{C_m}{\tan\beta}$ (6)

Simulated total head rise:

$H_{rise} = \dfrac{\overline{P_{2total}} - \overline{P_{1total}}}{\rho g}$ (7)

B. Collector design

For this study, the collector is built as a concentric casing followed by a partial volute that discharges into a diffuser. The combined casing is started by designing an annular collector over 180° followed by a volute leading the fluid into the discharge diffuser. Shape of collector is shown in Fig. 2.
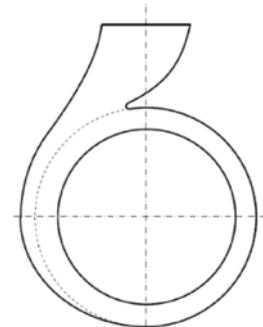

Fig. 2. Shape of collector

III. BASIC MATHEMATICAL EQUATION OF THE MODEL

For three-dimensional incompressible and unsteady flow, the continuity and momentum equations in the rotating coordinate system are as follows:

Continuity equation: $\dfrac{\partial \rho}{\partial t} = \vec{\nabla} \cdot \rho \vec{V}$ (8)

Momentum equation:

$$\rho \frac{d\vec{V}}{dt} + \vec{\nabla}P = \rho\vec{g} + \mu\left(\nabla^2 \cdot \vec{V}\right) - 2\rho\vec{\omega}\times\vec{V} - \rho\vec{\omega}\times\left(\vec{\omega}\times\vec{r}\right)$$
(9)

IV. ANALYSIS OF 3D IN THE IMPELLER

The analysis for the double-acting impeller with straight radial blades was based on the following design details: a volume flow rate of 33.5 m³/h, head of 100 m, rotational speed of 2950 1/min, and specific speed of 9. A head coefficient of 1.4 and a flow coefficient of 5.9 x 10⁻³ were established. The analysis starts with grid generation and refinement on a single channel domain of Fig 3. All the grids generated were hexahedral structured grids with approximately 29,870 nodes as shown in Fig.4. The inlet and outlet flow of a single channel of simulation domain were shown in Fig.5. The numerical flow

field calculation was performed using CFX 13 code. The main parameters are presented in Table 1 and the analyzed parameters were shown in Table 2.
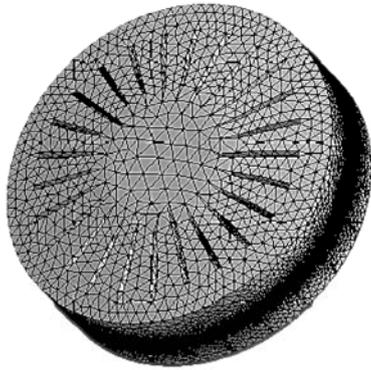

Fig. 3. Domain of impeller

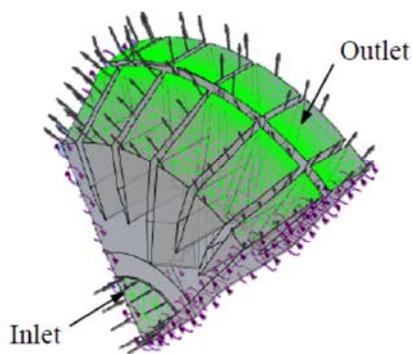Fig.4. Computational grids for a single channel of the impeller

Fig.5. Inlet and outlet flow of a single channel of simulation domain

Table 1: Geometrical parameters of double acting impeller with straight radial blades and collector:

$$n_q = 9$$

Parameter	Value	Description
Impeller		
b_2	60 mm	Impeller outlet width
b_1	65 mm	Impeller inlet width

D_2	230 mm	Impeller outlet Diameter
$\beta_1 = \beta_2$	90 deg	Angle of blade at inlet and outlet
Ns	20	Short blade number
Nl	5	Long blade number
Collector		
D_3	244 mm	Base collector diameter
b_3	75 mm	Collector width

Table 2: Simulation parameters

Parameters	CFX 13
Flow simulation domain	One impeller flow channel
Grid	Structured
Fluid	Water at 25 °C
Inlet	Total pressure = 101325 Pa
Outlet	Mass flow rate
Wall	No slip
Turbulence model	$k - \varepsilon$
Turbulence intensity	5%
Maximum residual convergence	10^{-4} (RMS)

V. RESULTS AND DISCUSSION

Based on this study, the Q-H curve of an impeller can be determined as shown in Fig. 6. The head value determined at the design point is 100 m. Hence, Fig. 6 shows that the total head rise value of 98.80 m is close to the designed head. Fig. 6 shows that the Q-H curve rises continuously toward shutoff as the flow rate is reduced.
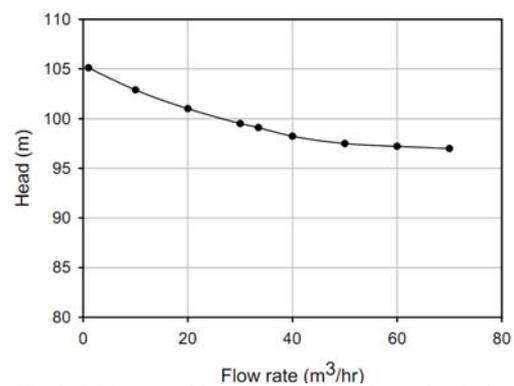

Fig.6. Q-H curve of impeller obtained from simulation

A. Variation of the impeller inlet width
Considering the streamline occured in blade passages of a single channel of impeller with the impeller inlet width of $b_1 = 65$ mm, there is a lot of circulation close to the surface of blades in every blade passages. This circulation causes losses, which leads to reduced the performance of the impeller.

The impeller was re-designed by fixing the values of every parameters and adjusting only the impeller inlet width (b_1). It was found that, when the impeller inlet width (b_1) changes from 65 mm to 70 mm, there is still circulation in every blade passages, but it becomes smaller. The circulation can be observed from streamline occured in a single channel of impeller as shown in Fig. 7 and Fig. 8. It was also found that water does not flow fully in the blade passages. Calculations show that the head at the design point is 99.89 meters.

Figure 9 shows a comparison of the Q-H curves before and after adjusting the impeller inlet width. It can be seen that the adjustment of the impeller inlet width causes reduced circulation in the blade passages and water can flow more fully in the blade passages. Hence, the performance of impeller much better.
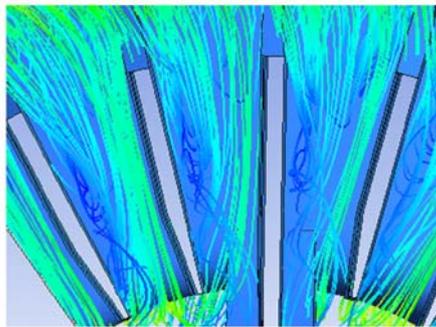

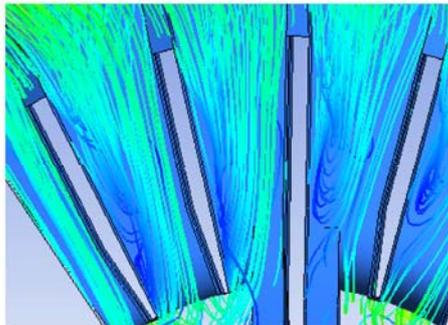**Fig. 7. Streamline at impeller inlet width, b^1=65 mm before refinement**

Fig. 8. Streamline at impeller inlet width, b^1=70 mm after refinement
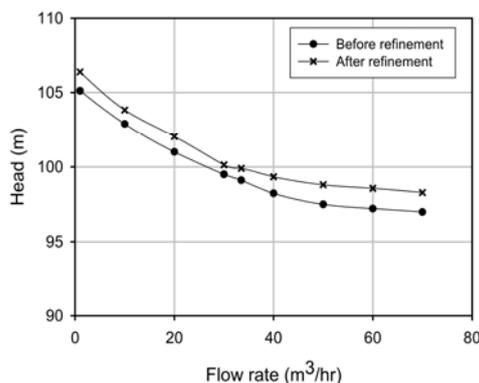

Fig. 9. Q-H Curve before and after impeller refinement

B. Effect of velocity distribution on the blade passages of the impeller

Considering the meridian velocity distribution of the absolute velocity from the hub to the shroud at the impeller inlet (C_{1m}) and outlet (C_{2m}), it was found that the meridian velocity at the impeller inlet and outlet are uniform at both the front side and the rear side as shown in Fig 10 and Fig. 11. However, the meridian velocity at the rear side is less than that at the front side. It is noticeable that the meridian velocity distribution of the absolute velocity at the out let (C_{2m}) at the front side overlaid that at the rear side.

The circumferential component of the absolute velocity from the hub to the shroud at the impeller inlet (C_{1u}) and outlet (C_{2u}) can be observed from Fig. 12 and Fig. 13. It was found that in case of the circumferential component of the absolute velocity at the impeller inlet (C_{1u}) is not equal to zero, this suggests that there is swirl or pre-rotation in the flow at the impeller inlet.
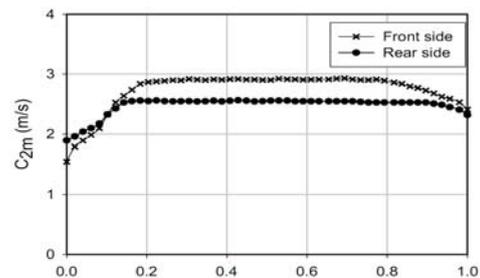

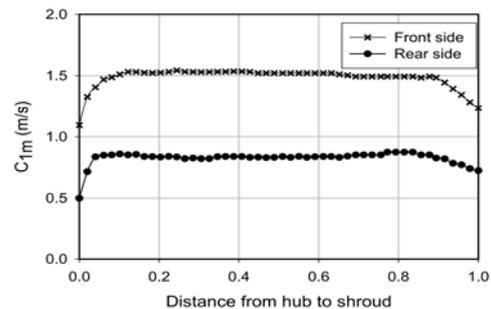**Fig. 10. Meridian component of absolute velocity distribution at the impeller outlet**

Fig. 11. Meridian component of absolute velocity distribution at the impeller inlet
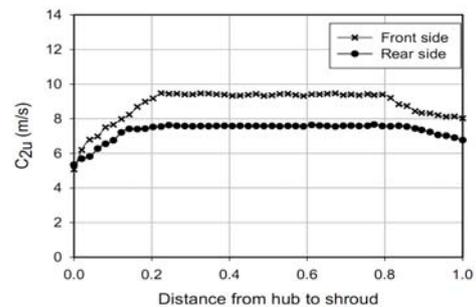

Fig. 12. Circumferential component of absolute velocity distribution at the impeller outlet
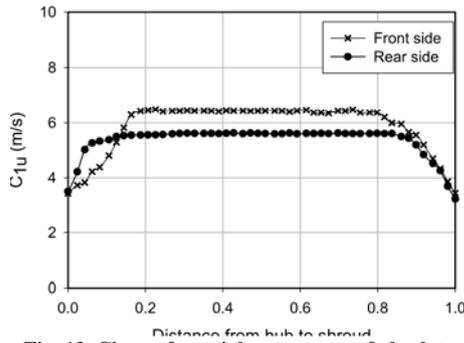
Fig. 13. Circumferential component of absolute velocity distribution at the impeller inlet

C. Impeller-collector 3D flow simulation

A 3D view of the collector is shown in Fig. 14. All the grids of the collector were hexahedral structured grids with approximately 121,848 nodes. The original configuration of the outlet collector was essentially extended for numerical reasons since convergence problems and related flow instabilities are prevented. Swirling flow appeared in the impeller inlet. Therefore, it was necessary to extend the impeller inlet upstream as shown in Fig. 15. Due to the change between the reference frame of the rotating impeller and the static collector, the interaction of the impeller-collector was simulated using the frozen-rotor interface model. The interface between impeller domain and collector domain is shown in Fig. 16.

The simulation parameters for the impeller-collector assembly can be summarized as shown in Table 3. An image of the internal flow inside the impeller-collector assembly given by the simulation enables us to analyze and understand this complex phenomenon. The fluid dynamics calculations for the impeller-collector assembly using CFX 13 code gives the total head rise, which can be used to calculate heads at various flow rates using equation 7 . The Q-H curve can be plotted as shown in Fig. 17. The total head rise at the design flow rate is 98.0 m, which is lower than the head at the design point of 100 m. The Q-H curve rises continuously toward shutoff as the flow rate is reduced, as in the case of the isolated impeller. A change in the Q-H curve cannot be dropping toward shutoff or does not have a saddle characteristic. A comparison of the graphs reveals that the Q-H curve of the impeller-collector assembly is slightly lower than that of the isolated impeller. It should be noted that the flow at both the front side and the rear side of the blades causes the axial thrust to drop.

Figures 18, 19, and 20 show the velocity field and pressure distribution at various Q/Q_{design} values.

Figure 18 shows the pressure field at the design point of $Q/Q_{design} = 1.0$. It can be seen that the pressure distribution and velocity field around the impeller periphery is uniform. Considering the pressure

distribution at a lower point than the design point of $Q/Q_{design} = 0.6$ and higher than the design point of $Q/Q_{design} = 1.5$, it was found that the pressure near the tongue was slightly higher than the pressure at the design point. The velocity field outside the design point causes a vortex or circulation at the rear side of the diffuser. This could be improved by re-designing the diffuser.
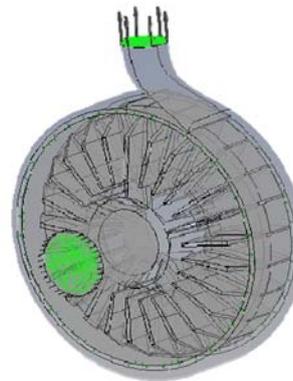

Fig. 14. Domain of collector

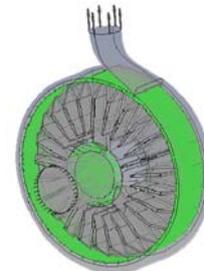
Fig. 15. Extension impeller inlet and collector outlet

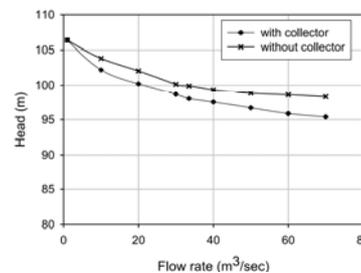**Fig. 16. Interface between impeller domain and collector domain**

Fig. 17. Q-H Curve of impeller-collector assembly

VI. CONCLUSION

This study analyzed the flow simulation in a double-acting isolated impeller and in an impeller-collector

assembly using CFX 13 code. The study begins with an isolated impeller. The mathematical model used is the $k - \varepsilon$ model with 29,870 nodes on the blade passage. The resulting Q-H has stable characteristics. In the case of the impeller-collector assembly, more computational domains are needed at the impeller inlet and the collector outlet. The interface between the impeller and the extended duct at inlet and between the impeller and the collector is a frozen-rotor model. The Q-H curve has similar stable characteristics as the isolated impeller, with a slightly lower graph due to losses in the collector. The circumferential component of the absolute velocity at the inlet (C_{1u}) is not equal to zero due to the occurrence of pre-rotation or swirl. The analysis of flow in the blade passage shows circulation in nearly every blade passages or channels. However, widening the impeller inlet width reduces the circulation. In the impeller-collector assembly, there is circulation at the rear side of the diffuser when Q / Q_{design} is both lower and higher than 1.0. This study experiments with a double-acting impeller with straight radial blades centrifugal pump that could be manufactured for commercial use as mentioned in references [3] and [4].

ACKNOWLEDGMENT

NOMENCLATURE

b_1 : Width of impeller inlet (mm)

b_2 : Width of impeller outlet (mm)

b_3 : Width of collector (mm)

C_{1u} : Circumferential component of absolute velocity at
    inlet (m/s)

C_{2u} : Circumferential component of absolute
    velocity at outlet (m/s)

C_{1m} : Meridian component of absolute velocity at
    inlet (m/s)

C_{2m} : Meridian component of absolute velocity at outlet
        (m/s)

D_1 : Diameter of impeller at inlet (mm)

D_2 : Diameter of impeller at exit (mm)

D_3 : Base collector diameter

g : Gravitational acceleration (m/s^2)

H : Design head (m)

$H_{rise:}$: Simulated total head rise (m)

Ns : Short blade number

Nl : Long blade number

k : Turbulence kinetics energy

n : Speed (rpm)

n_q : Specific speed (1/min)

P_{1total} : Total pressure at impeller inlet (N/m^2)

P_{2total} : Total pressure at impeller outlet (N/m^2)

Q : Volume flow rate (m^3/s)

u : Circumferential impeller velocity (m/s)

β_1 : Angle of blade at inlet (deg)

β_2 : Angle of blade at outlet (deg)

ε : Turbulence eddy Dissipation

ρ : Density (kg/m^3)

ω : Angular velocity (rad/s)

ϕ : Flow Coefficient

ψ : Head Coefficient

REFERENCES

[1] M.Asujie, F. Bakir, S. Kouidri, F.Kenyery and R. Rey, Numerical Modelization of the Flow in Centrifugal Pump: Volute Influence in Velocity and Pressure Fields, International Journal of Rotating Machinery, 3, 2005, 244-255.

[2] F. Muggli, P. Holbein, and P. Dupont, CFD calculation of a mixed flow pump Characteristic from shutoff to maximum flow Proceedings of the ASME Fluids Engineering Division Summer Meeting (FED01), New Orleans, La, USA, June, 2001, Paper FEDSM01-18072.

[3] Cropper M, Dupont P, Parker J: Low flow – high pressure, Sulzer Technical Review, 2005.

[4] J.F. Guelich, Centrifugal Pumps, 2nd Edition, Springer, Berlin, (2010).

[5] E. Blanco-Marigorta, J. Fernandez-francos, J.L. Parrondo-Gayo and C. Santoria-Marros, umerical simulation of centrifugal pumps, Proceedings of the ASME Fluids Engineering Division Summer Meeting (FED00), Boston, Mass USA, June, 2000, Paper FEDSM00- 11162.

[6] J. Gonzalez, J. Fernandez-Francos, E Blanco and C. Santolaria-Marros, Numerical Simulation of the dynamic effects due to impeller-volute interaction in a centrifugal pump, Transactions of the ASME, Journal of Fluids Engineering, 124, 2002, 348-355.

[7] J.L. Parrondo-Gayo, J. Gonzalez-Perez and J. Fernandez-Francos, The effect of operating point on the pressure fluctuations at the blade passage frequency in the volute of a centrifugal pump, Transactions of the ASME, Journal of Fluids Engineering, 124, 2002, 784-794.

[8] F.Gu, A. Engeda, M Cave and J.L. Di Liberti, A Numerical investigation on the volute/diffuser interaction due to the axial distortion at the impeller exit, Transactions of the ASME, Journal of Fluids Engineering, 123, 2001, 475-483.
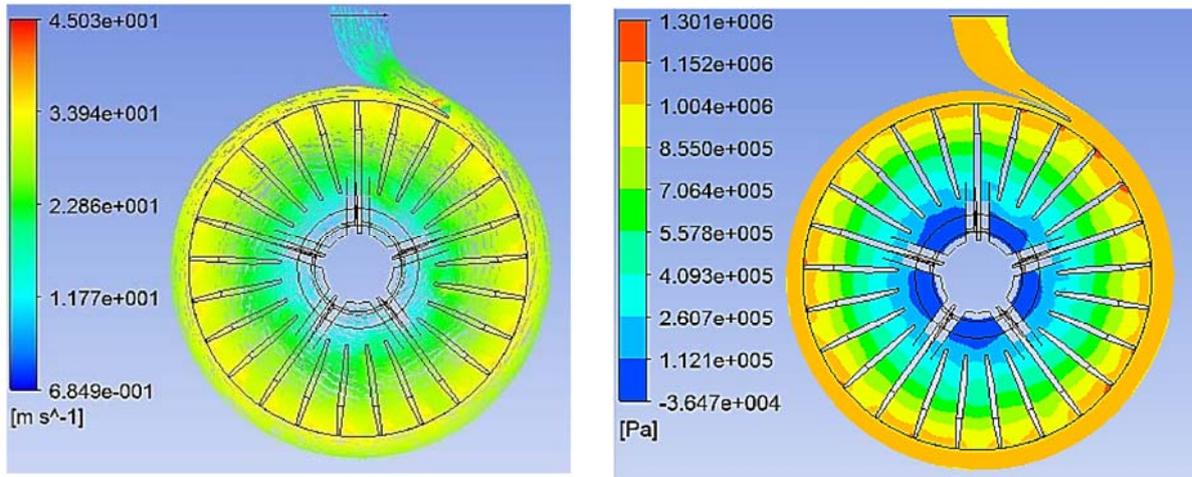
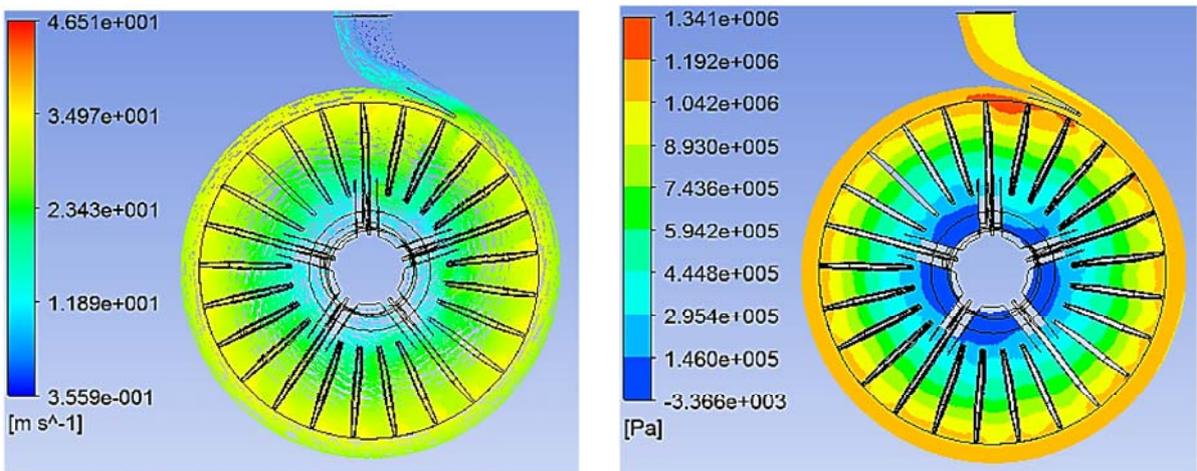Fig. 18. Velocity field and pressure field at $Q/Q_{design} = 1.0$

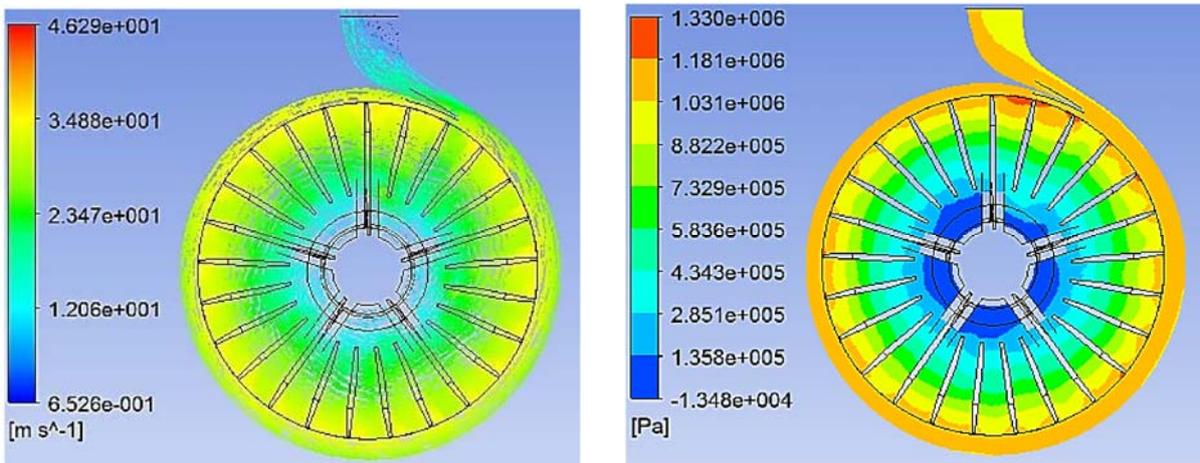Fig. 19. Velocity field and pressure field at $Q/Q_{design} = 0.6$

Fig. 20. Velocity field and pressure field at $Q/Q_{design} = 1.5$

❖ ❖ ❖